



A NOVEL COMPUTATIONAL APPROACH FOR CALCULATING SAGITTAL PLANE UROGENITAL KINEMATICS FROM DYNAMIC 2D ULTRASOUND

Catriona Czynnyj¹, Dr. Michel Labrosse¹, Dr. Linda McLean²

1. Faculty of Engineering, University of Ottawa

2. Faculty of Health Sciences, University of Ottawa

INTRODUCTION

Stress urinary incontinence (SUI) is defined as the leakage of urine during tasks that increase intra-abdominal pressure (IAP), such as coughing¹. SUI accounts for 50% of all incontinence cases^{1,2} and affects up to half of all women at some point in their lives^{1,2}. In Canada, urinary incontinence (UI) costs \$8.5 billion annually³ and has countless effects on quality of life⁴. While SUI is likely due to concurrent failures in urethral sphincter function⁵, urethral support^{6,7}, and pelvic floor muscle (PFM) mechanics^{5,8}, the exact mechanism is not well understood.

In order to investigate the pathomechanics associated with SUI, sagittal plane transperineal ultrasound (TPUS) has recently gained popularity. TPUS has demonstrated differences in urogenital kinematics between women with and without SUI while they perform coughing and Valsalva maneuvers⁶⁻⁸. However, dynamic TPUS imaging is vulnerable to probe translation and rotation in 3D space occurring throughout the task. The resulting measurement error is difficult to detect because there is only one visible bony landmark, the pubic symphysis (PS), and often only a small fraction of the PS remains visible throughout the task.

Two key papers have presented methods to quantify urogenital kinematics using anatomical landmarks in the mid-sagittal plane. Shek and Dietz⁷ described a urethral mobility profile (UMP) where the net displacement of six points along the urethra (from the bladder neck (BN) to the external urethral meatus) were visualized at peak Valsalva. One limitation of this method is the use of a coordinate system that is based on the location of the dorsocaudal

margin of the PS. However, probe translation and rotation can affect the orientation of the PS relative to the structures of interest, in this case the urethra. Thus rotation of this coordinate system could be indicative of probe motion or simply poor alignment of the axes. Additionally, the apparent location of the external urethral meatus is particularly affected by transducer pressure, which can change markedly throughout tasks such as coughing and Valsalva maneuvers.

Separately, Peng et al⁸ investigated the motion of the anorectal angle (ARA) in women with SUI while they coughed. Peng et al⁸ provided visual feedback during image acquisition, using Flock of Birds (FOB) instrumentation, to limit probe rotation to less than $\pm 5^\circ$, assuming that this rotation would minimally impact measurements. To address probe translation, they created a coordinate system with the y-axis parallel to the urethra and the x-axis intersecting the most dorsal point of the PS. They then subtracted translational probe motion by comparing the position of the PS between frames. An identical procedure was used to account for the motion of the ARA with the inclusion of a weighting factor, due to soft tissue deformation of the landmark. The rationale for the precise weighting factor was not reported. The method of Peng et al⁸ also has limitations. The alignment of the y-axis is difficult to determine in practice because the urethra is often curved and can deform during dynamic tasks. As well, though probe rotation was constrained via the FOB, the magnitude of error due to this rotation was not investigated.

In order to understand the biomechanical factors associated with SUI, valid and reliable measurements are required. TPUS is a potential

solution, but it must accurately describe urogenital biomechanics. We have developed a novel computational method to compensate for in-plane translation and rotation error during dynamic TPUS, allowing us to study urogenital dynamic tasks known to cause urine leakage.

METHODS

All computational methods were executed using Matlab 2015b (Mathworks, Natick, MA, USA). A video player was created to load and play .avi files generated by the ultrasound software, a General Electric Voluson-i portable ultrasound console. The PS was selected to track probe motion because it is the only non-deforming landmark on the TPUS images, and thus PS motion actually reflects motion of the patient with respect to the TPUS probe. The last frame recorded before the task motion began was defined as the reference frame.

In order to track object motion, we chose to define a 2D coordinate system (CS) that could be rebuilt in every frame. In order to build the CS the user traces an outline of the posterior surface of the PS (*Figure 1*). In each frame, the PS trace from the reference frame is duplicated, translated, and/or rotated to align maximally with the PS. Since the PS is ideally always the same size and shape, the CS can always be rebuilt in an identical manner. The identification of the PS and other relevant landmarks

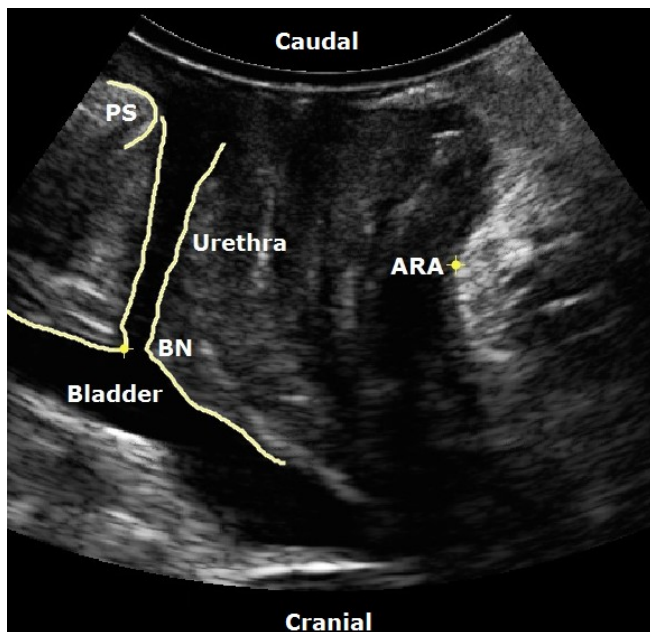


Figure 1: Identification of PS and ARA on a sagittal plane TPUS during cough task. PS refers to the pubic symphysis, ARA refers to the ano-rectal angle, and BN refers to the bladder neck.

(bladder neck, ARA, urethra; *Figure 1*) on each frame are the only tasks required of the user. From these landmarks, several morphologic and kinematic features are computed automatically. As an example, motion of the ARA during a cough task will be described here.

In the reference frame, the x-axis is defined as a line running from the antero-caudal end of the PS to the center of the PS trace. The y-axis intercepts the PS center point and runs perpendicular to the x-axis, and this is referred to as the Global coordinate system (GCS). In all other frames, these same axes are defined as the LCS. For each frame, a transformation matrix is built to convert the anatomical landmarks from their LCS to the GCS. This allows landmark motion parameters (displacement, velocity, acceleration) to be computed by the software.

The transformation matrix for each frame is constructed as in (1), where i and j are the x and y LCS unit vectors, I and J are the GCS x and y unit vectors and p and q are the x and y displacements between the center points of the PS trace from the LCS to the GCS.

$$TR = \begin{bmatrix} i \cdot I & i \cdot J & p \\ j \cdot I & j \cdot J & q \\ 0 & 0 & 1 \end{bmatrix} \quad (1)$$

Thus the motion of a landmark in any given frame can be described in the GCS, as in (2), where the prime notation indicates the LCS and non-prime indicates GCS.

$$\begin{bmatrix} x \\ y \\ 1 \end{bmatrix} = \begin{bmatrix} i \cdot I & i \cdot J & p \\ j \cdot I & j \cdot J & q \\ 0 & 0 & 1 \end{bmatrix} \begin{bmatrix} x' \\ y' \\ 1 \end{bmatrix}$$

$$GC = R \quad LC \quad (2)$$

Once the ARA position in all relevant frames has been converted to the GCS, the ARA displacement can be determined with reference to *Figure 2*.

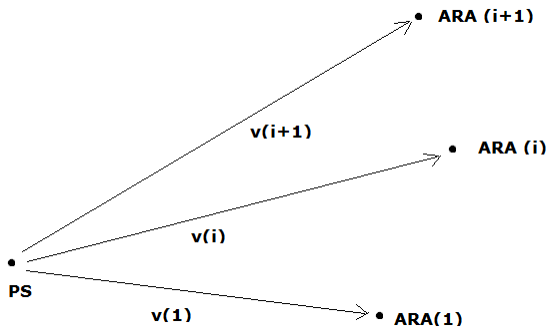


Figure 2: Motion of the ARA with respect to the PS over time. The X-Y position of the posterior-most point of the PS is represented by PS. The X-Y position of the ARA at times (i) and (i+1) are represented by vectors ARA(i) and ARA(i+1), respectively. The vectors v(i) and v(i+1) represent the position of the ARA with respect to the PS at times (i) and (i+1), and the vector v(1) denotes the initial position of the ARA with respect to the PS. ARA(i)_{disp} is then the displacement of the ARA with respect to its initial position at time (i).

After the transformation matrices have been applied, the PS is static and thus the displacement of the ARA at time (i) can be found simply as follows (3):

$$\mathbf{v}(i) = \mathbf{ARA}(i) - \mathbf{PS}$$

$$\mathbf{ARA}(i)_{\text{disp}} = \mathbf{v}(i) - \mathbf{v}(1) \quad (3)$$

Trajectories are low pass filtered (dual pass, 4th order, Butterworth) with cutoff frequency set to the capture rate for the ultrasound video. Capture rates for the GE Voluson-i vary depending on the number of frames captured.

For initial software testing, a subset of data was used from an ongoing study that has received approval from the local ethics board. All women provided written informed consent prior to participating, and it is expected that the software algorithm will be used for image processing in the larger study.

TPUS data were acquired while women with SUI performed a series of dynamic tasks including maximum effort coughs. All images were acquired using a GE Voluson i ultrasound system (GE Healthcare Austria GmbH & Co OG, Zipf, Austria) in 2D real time B-mode, interfaced with an 8- to 4-MHz curved array 3D transducer. The transducer was placed transperineally with the main transducer axis oriented in the mid-sagittal plane, and the volume acquisition angle was set to its maximum at 85 degrees. Imaging was

performed after bladder emptying. Participants were in supine with their hips slightly abducted and flexed approximately 30 degrees, knees flexed approximately 30 degrees, and feet supported in stirrups. ARA motion throughout the task is described to allow direct comparison with Peng et al⁸, whose work provides the most thorough analysis of urogenital kinematics in the current literature.

RESULTS

Representative data from a female patient age 37 years, BMI 24.2 kg/m² who reports moderate SUI, with 3.83g leakage on a standardized 30 minute pad test⁹ and 7 episodes of urine leakage over a 3 day voiding diary⁹ is presented.

The displacement of the ARA is depicted on the polar plot in *Figure 3*. In our participant, the ARA moves antero-caudally during the cough task, The ARA reaches its peak displacement at 16.8mm from its initial position, at an angle of 259°. The ARA then

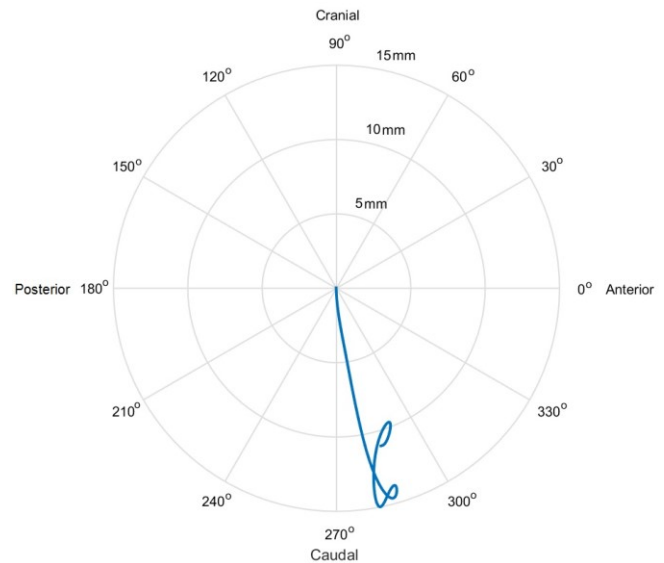


Figure 3: Displacement (trajectory) of the ARA in the sagittal plane during a double barrel cough performed by a female with moderate SUI.

begins to return towards its initial position, but changes direction again and moves more caudally. The final position of the ARA is 10.92mm from its initial position at an angle of 255°.

DISCUSSION

While data from a single patient are not adequate to compare outcomes, the motion of the ARA seen in this participant suggests that the PFM's contracted sufficiently to move the ARA closer to the PS (anteriorly) during the cough, but not sufficiently to resist the caudal forces induced on them through the increase in intra-abdominal pressure during the cough. Additionally, our analysis captured the double barrel nature of the cough, seen in the two peaks in *Figure 3*. During data collection, our technician did not use any tool to track probe motion, and we did not need to determine a weighting factor to account for tissue distortion.

Unlike the results of the SUI subjects seen in Peng et al⁸, the ARA in this participant moved antero-caudally, not postero-caudally; it did not return to its initial position; and experienced larger peak magnitudes of displacement. There are a variety of reasons that could explain this phenomenon including methodological differences (use of a weighting factor and averaging data over four repeated analyses), differences in task performance, and the multifactorial nature of the SUI condition. The small sample size (n=9) of women with SUI described by Peng et al⁸ indicates that their results may not be an accurate representation of ARA displacement in women with SUI.

While our methods may improve on other published approaches, there are still limitations with this work. Ideally, our software would be based on 4D TPUS and include concurrent optimization of the image even when out-of-plane motion occurs. However, our 4D ultrasound system, like most, does not have 4D acquisition rates that are adequate to capture dynamic motion, such as tracking the ARA or urethral motion throughout a cough. With the rapid evolution of high speed ultrasound over recent years, this may soon be a possibility, and our algorithms have been developed such that image optimization through volume rotation is easily incorporated. Additionally, rotation correction in our algorithm occurs about the midpoint of the PS trace, not the true center of probe rotation. We are currently investigating the ramifications of this simplified approach.

Mathematically, our methods provide a simple, thorough, accurate compensation for probe motion. Our software can provide a robust analysis of urogenital kinematic data, including angular kinematics, velocities, and accelerations. Our next steps are to investigate the implications of center of rotation, test the validity of the algorithm by imaging a custom gel model and evaluate the inter- and intra-user reliability of this software on a set of images.

ACKNOWLEDGEMENTS

The authors would like to thank Dr. Ryan Graham for his contributions to the development of the algorithms.

REFERENCES

1. Reynolds, W. S., Dmochowski, R. R. & Penson, D. F. Epidemiology of stress urinary incontinence in women. *Curr. Urol. Rep.* **12**, 370–376 (2011).
2. Bettez, M. et al. 2012 update: Guidelines for adult urinary incontinence collaborative consensus document for the Canadian Urological Association. *J. Can. Urol. Assoc.* **6**, 354–363 (2012).
3. The Impact of Incontinence in Canada A Briefing Document for Policy-Makers. (2014).
4. Abrams, P., Smith, A. P. & Cotterill, N. The impact of urinary incontinence on health-related quality of life (HRQoL) in a real-world population of women aged 45-60 years: Results from a survey in France, Germany, the UK and the USA. *BJU Int.* **115**, 143–152 (2015).
5. DeLancey, J. O. L. et al. Vaginal Birth and De Novo Stress Incontinence. *Obstet. Gynecol.* **110**, 354–362 (2007).
6. Pirpiris, A., Shek, K. L. & Dietz, H. P. Urethral mobility and urinary incontinence. *Ultrasound Obs. Gynecol* **36**, 507–511 (2010).
7. Shek, K. L. & Dietz, H. P. The urethral motion profile: a novel method to evaluate urethral support and mobility. *Aust. N. Z. J. Obstet. Gynaecol.* **48**, 337–42 (2008).
8. Peng, Q., Jones, R., Shishido, K. & Constantinou, C. E. Ultrasound evaluation of dynamic responses of female pelvic floor muscles. *Ultrasound Med. Biol.* **33**, 342–52 (2007).
9. McLean, L. et al. Pelvic floor muscle training in women with stress urinary incontinence causes hypertrophy of the urethral sphincters and reduces bladder neck mobility during coughing. *Neurourol. Urodyn.* **32**, 1096–1102 (2013).